JACS
JOURNAL OF THE AMERICAN CHEMICAL SOCIETY
Communication
pubs.acs.org/JACS

Controlled Growth of Atomically Thin In_2Se_3 Flakes by van der Waals Epitaxy

Min Lin,[†] Di Wu,[†] Yu Zhou,[†] Wei Huang,[‡] Wei Jiang,[†] Wenshan Zheng,[†] Shuli Zhao,[†] Chuanhong Jin,[‡] Yunfan Guo,[†] Hailin Peng,*[,†] and Zhongfan Liu*[,†]

[†]Center for Nanochemistry, Beijing National Laboratory for Molecular Sciences (BNLMS), State Key Laboratory for Structural Chemistry of Unstable and Stable Species, College of Chemistry and Molecular Engineering, Peking University, Beijing 100871, P. R. China

[‡]State Key Laboratory of Silicon Materials, Key Laboratory of Advanced Materials and Applications for Batteries of Zhejiang Province, Department of Materials Science and Engineering, Zhejiang University, Hangzhou 310027, P. R. China

Supporting Information

ABSTRACT: The controlled production of high-quality atomically thin III−VI semiconductors poses a challenge for practical applications in electronics, optoelectronics, and energy science. Here, we exploit a controlled synthesis of single- and few-layer In_2Se_3 flakes on different substrates, such as graphene and mica, by van der Waals epitaxy. The thickness, orientation, nucleation site, and crystal phase of In_2Se_3 flakes were well-controlled by tuning the growth condition. The obtained In_2Se_3 flakes exhibit either semiconducting or metallic behavior depending on the crystal structures. Meanwhile, field-effect transistors based on the semiconducting In_2Se_3 flakes showed an efficient photoresponse. The controlled growth of atomically thin In_2Se_3 flakes with diverse conductivity and efficient photoresponsivity could lead to new applications in photodetectors and phase change memory devices.

The isolation of graphene in 2004 has triggered a research boom in two-dimensional (2D) crystals with exceptional properties and new applications contrast to their bulk counterparts.[1,2] So far, a variety of 2D crystals have been explored, including semimetallic graphene,[1] insulating hexagonal boron nitride,[3,4] V−VI topological insulator (Bi_2Se_3, Bi_2Te_3, and Sb_2Te_3),[5−8] and semiconducting transition-metal dichalcogenides (MoS_2, WS_2, etc.).[9] Indium selenide (In_2Se_3), an intriguing III−VI binary chalcogenide with crystalline polymorphism and diverse electronic properties, is considered as a promising material for the applications in photovoltaic devices,[10,11] optoelectronics,[12,13] phase change memory,[14,15] and ionic batteries.[16] In_2Se_3 compound occurs at least in five different crystalline modifications,[17−19] which can be divided into the layer-structured phase and the phase with vacancy ordered in a screw form,[17] although the accurate structures are still under question. We and others have recently synthesized layer-structured In_2Se_3 nanowires and nanoribbons via a metal nanoparticle-catalyzed vapor−liquid−solid process.[20−23] The In_2Se_3 nanowire and nanoribbon were found to exhibit the simple hexagonal lattice structure or superlattice structure, which correspond to a semiconducting or metallic behavior, respectively.[21,22] Most recently, highly crystalline In_2Se_3 nanowires were assembled in photodetectors with fast, reversible, and stable photoresponse characteristics. The remarkably high photosensitivity and quick photoresponse may be attributed to the good crystalline quality and large surface-to-volume ratio of the nanowire.[13] On the other hand, 2D materials are more compatible with traditional microfabrication techniques and are easily fabricated into complex structures and 2D heterostructures to meet the needs of new electronic and optoelectronic devices.[9,24] The controlled production of high-quality atomically thin In_2Se_3 layers is critical to their practical application in electronics and optoelectronics.

Here we first report a facile approach for the synthesis of atomically thin In_2Se_3 flakes with a thickness, position, and orientation control by van der Waals epitaxy.[25,26] The crystalline phase can be also controlled to a certain extent by tuning the growth condition. Moreover, In_2Se_3 flakes with different crystal structures show a great diversity in the conductivity and efficient photoresponsivity, which may open up opportunities for 2D crystals of chalcogenides in a range of novel nanoelectronics and optoelectronics.

Figure 1A shows a schematic drawing of layered α-phase In_2Se_3 grown in the space group $P6_3$ on a layered substrate. α-In_2Se_3 is made up of planar quintuple layers (QLs) with strong in-plane covalent bonding and weak out-of-plane van der Waals interactions. Each QL consists of Se−In−Se−In−Se with the thickness of ~1 nm.[17] The van der Waals epitaxy growth[25,26] of large-area, high-quality In_2Se_3 flakes were carried out in a setup similar to our previous synthesis of nanowire and nanoribbons (See Methods in Supporting Information (SI)).[20,21] In_2Se_3 powder (99.99%, Alfa Aesar) was placed at the hot center of the tube furnace heated to 690−750 °C. The vapor was carried downstream by 30−200 sccm Ar gas, and In_2Se_3 flakes were deposited on the substrate placed 7−12 cm away from heating center, where the temperature ranges from 670 to 540 °C. Since van der Waals epitaxy allows defect-free epilayer to grow on layered substrates even with a large lattice mismatch, we used two kinds of layered substrates including conductive graphene and insulating fluorophlogopite mica ([$KMg_3(AlSi_3O_{10})F_2$]) as the growth substrate. Figure 1B,C shows typical scanning electron

Received: June 24, 2013
Published: August 26, 2013

 © 2013 American Chemical Society

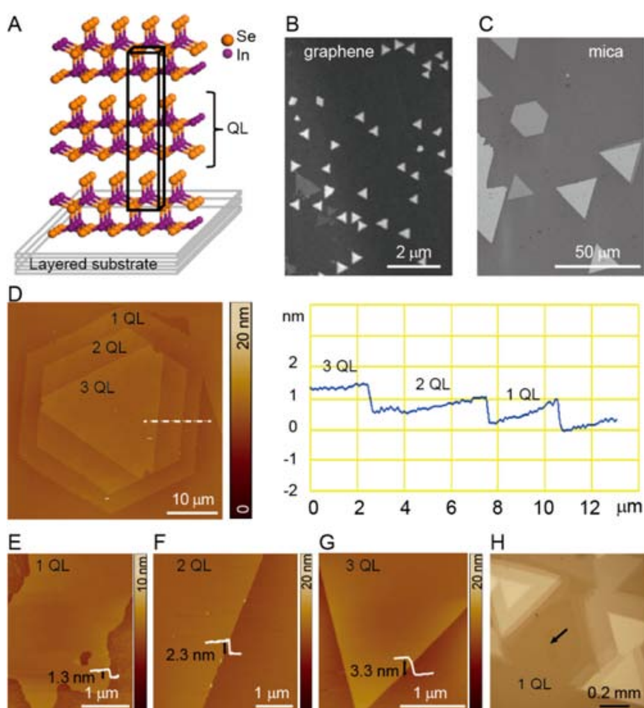

Figure 1. (A) Schematic drawing of layer-structured In_2Se_3 flakes grown on a layered substrate. (B,C) SEM images of In_2Se_3 flakes grown on graphene and fluorophlogopite mica substrates, respectively. (D) AFM image and a height profile (corresponding to the dashed line-cut in the image) of a terraced In_2Se_3 flake with thicknesses of 1−3 QLs. The number of QLs is marked in AFM image and height profile. These flakes have multiple single QL steps, confirming layer-by-layer epitaxy modes. (E−G) AFM images of In_2Se_3 flakes with thicknesses of 1, 2, and 3 QLs, respectively. (H) Optical image of a large-area In_2Se_3 thin film with the single-layer region up to over 100 μm. The blank mica substrate is indicated by the black arrow.

microscopy (SEM) images of discrete In_2Se_3 flakes grown on a mechanically exfoliated graphene and cleaved fluorophlogopite mica, respectively. Triangular and hexagonal In_2Se_3 flakes with identical orientations were clearly seen on both substrates. The orientations of the In_2Se_3 flakes' edge were predominantly at multiples of ~60°, consistent with the 2D hexagonal lattice of the In_2Se_3 QL. The growth of orientation-defined In_2Se_3 flakes on different layered substrates reflects the essence of van der Waals epitaxy. Note that the size of In_2Se_3 flakes grown on mica is much larger than that grown on graphene, which may be caused by the atomically smooth surfaces over large areas of the cleaved mica substrate.

The thickness of synthesized atomically thin In_2Se_3 flakes is measured by atomic force microscopy (AFM), shown in Figure 1D as an example. Most of the flakes have terraced structures and atomically flat top facets with a uniform thickness across the lateral dimensions. The thickness of layered In_2Se_3 flakes can be tuned by adjusting the growth time, pressure, and Ar gas flow rate. For short growth time (5−40 min), the pressure of 50 Torr, and Ar gas flow of 40−60 sccm, we can obtain atomically thin layered In_2Se_3 flakes. Figure 1E−G shows typical AFM images of In_2Se_3 flakes with the uniform thickness of ~1.3, 2.3, and 3.3 nm, which can be denoted as 1 QL, 2 QLs and 3 QLs, respectively. Furthermore, we prepared continuous and large-area In_2Se_3 flakes or thin films with lateral dimensions extending from several micrometers up to hundreds of micrometers using longer growth time (40−90 min), Ar gas flow (40−100 sccm), and moderate pressure (20−50 Torr). As shown in the optical image (Figure 1H), the In_2Se_3 flake islands grown on the large-area In_2Se_3 thin films exhibit specific orientations, which conforms to a "layer-plus-island growth" mode.[27]

We have achieved a selective-area growth of atomically thin In_2Se_3 flakes by controlling the nucleation sites through the surface modification of the substrate. Figure 2A exhibits the schematic representation of the area-selective growth process. Mica substrates were first selectively modified by area-selective oxygen plasma etching followed by a conventional photolithography. After the poly(methyl methacrylate) (PMMA) photoresist was removed by acetone and subsequent annealing in air at 550 °C, as-pretreated mica substrates were loaded in the tube furnace for the In_2Se_3 flake growth. Since the chemical and morphological properties of mica are changed after oxygen plasma etching,[6] In_2Se_3 flakes prefer to nucleate and grow epitaxially on the intact mica region rather than the etched region. As shown in Figure 2B−D, atomically thin In_2Se_3 flakes and films with various patterns can be readily obtained according to the photolithography templates. From the AFM image shown in Figure 2E, the obtained nanostructures has a flat surface with a uniform thickness of down to 3 QLs, suggesting the high quality and controllability of In_2Se_3 flake grown by this selective-area method.

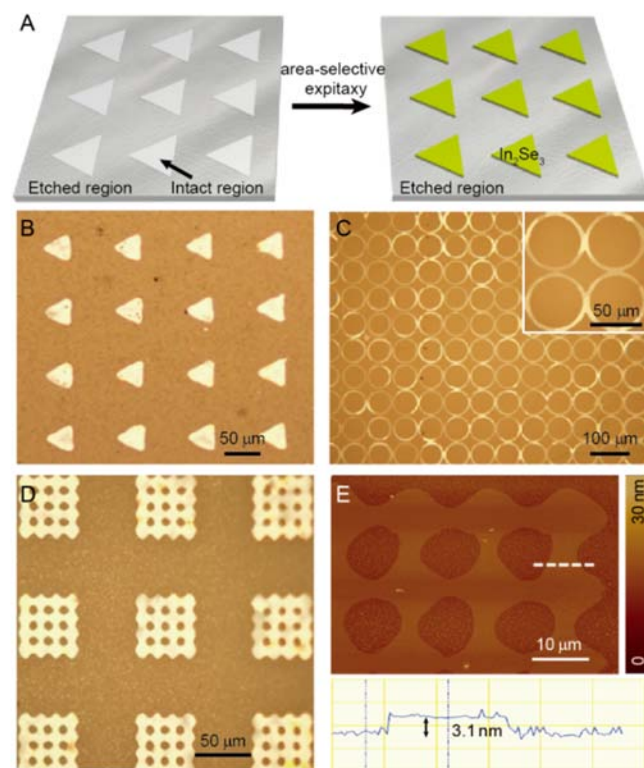

Figure 2. (A) Schematic representation of the growth process for selective-area growth of In_2Se_3 flakes on a modified mica substrate. (B−D) Optical images of triangular, annular, and perforated In_2Se_3 flake arrays obtained by the site-controlled growth, respectively. (E) AFM image and height profile of the perforated In_2Se_3 flake with the thickness of 3 QLs.

The atomically thin In_2Se_3 flakes with controlled morphologies can be faithfully transferred onto arbitrary substrates using a PMMA-mediated transfer technique,[28] which will facilitate the subsequent structural characterization and device fabrications

(Figure S1). After we transferred 2D In_2Se_3 flakes onto ultrathin porous carbon membranes, we have carried out transmission electron microscopy (TEM), selective area electron diffraction (SAED) and energy dispersive X-ray spectrometry (EDX) to investigate the crystal structures and chemical composition of In_2Se_3 flakes. EDX spectra and elemental maps (Figure S2) revealed that the as-grown flake consists of In and Se with an atomic ratio of 2:3 and homogeneous elemental distributions, confirming the chemical composition of In_2Se_3.

Atomically thin In_2Se_3 flakes provide a platform to investigate the microstructure and phase transition phenomena in a 2D system. In contrast to the bulk materials and thick nanoribbons of In_2Se_3 with complicated crystal phases,[17,22] two typical hexagonal crystal phases were observed in our atomically thin In_2Se_3 flakes: simple hexagonal (Figure 3A,B) and superlattice phase (Figure 3C,D). The high-resolution TEM (HRTEM) lattice fringes and spot pattern of SAED confirmed the single crystalline nature of the flakes. As shown in Figure 3A,B, the typical HRTEM image reveals expected hexagonal lattice fringes with a lattice spacing of 0.35 nm, consistent with the lattice spacing of (1−100) planes in the simple hexagonal phase. On the other hand, the superlattice phase has a periodicity of 1.40 nm and one period consists of four (1−100) planes (Figure 3C), which is further confirmed by the SAED pattern (Figure 3D) with the distance between two basic spots subdivided into four equal parts along the [1−100] direction. We also noticed that some regions of the atomically thin In_2Se_3 flake emerged with a coexistence of these two phases (Figure 3E,F). Interestingly, the cooling rate during In_2Se_3 flake growth can significantly influence the formation of crystalline phases. The simple hexagonal lattice phase can form by slow cooling rates (<5 °C/min) that may allow sufficient time for diffusion of atoms, whereas superlattice phase is usually formed by very high cooling rates (>100 °C/min).

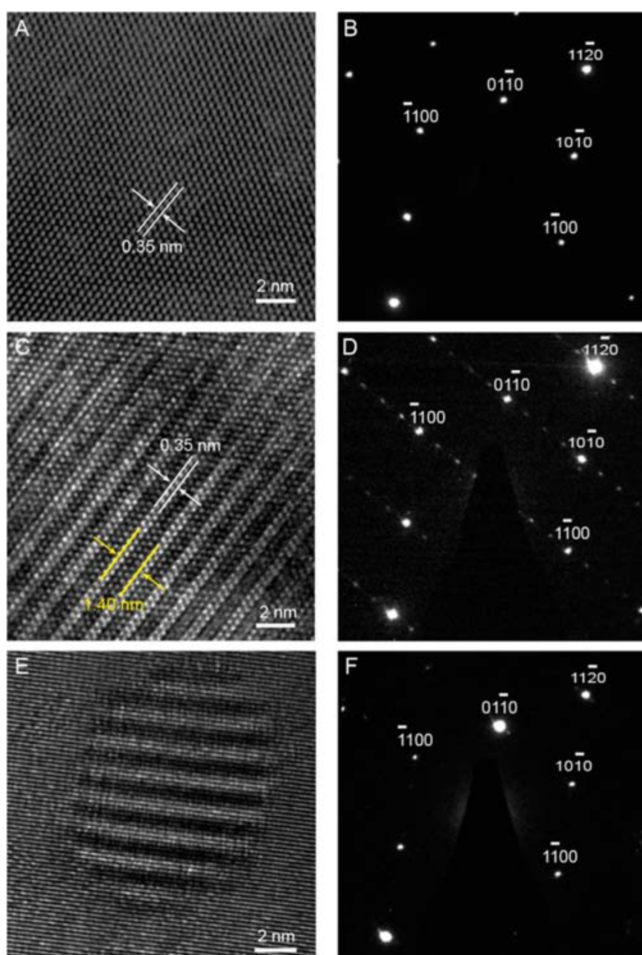

Figure 3. HRTEM images (left) and the corresponding SAED patterns (right). (A,B) Simple hexagonal lattice and (C,D) superlattice structures. (E, F) Mixed structure containing simple hexagonal lattice and superlattice.

The large-gain-size and atomically thin In_2Se_3 flakes greatly facilitated the fabrication of In_2Se_3 electronic and optoelectronic devices. We transferred discrete In_2Se_3 flakes grown on mica substrates onto SiO_2 (300 nm)/Si substrates. Metal contacts (25 nm In and 50 nm Au) were thermally evaporated onto the area defined by conventional electron beam lithography (EBL). The four-probe electronic transport measurements were carried out before extensive SEM imaging to avoid possible phase change (Figure S3). Two distinct structural phases, such as superlattice and simple hexagonal lattice as observed from the HRTEM images and the SAED patterns, formed in two types of flakes grown by rapid and slow cooling rate, respectively. Correspondingly, typical room-temperature $I-V$ characteristics of the two phases are shown in Figure 4A,B. The linear and symmetric curves suggested that ohmic contacts were formed at the source

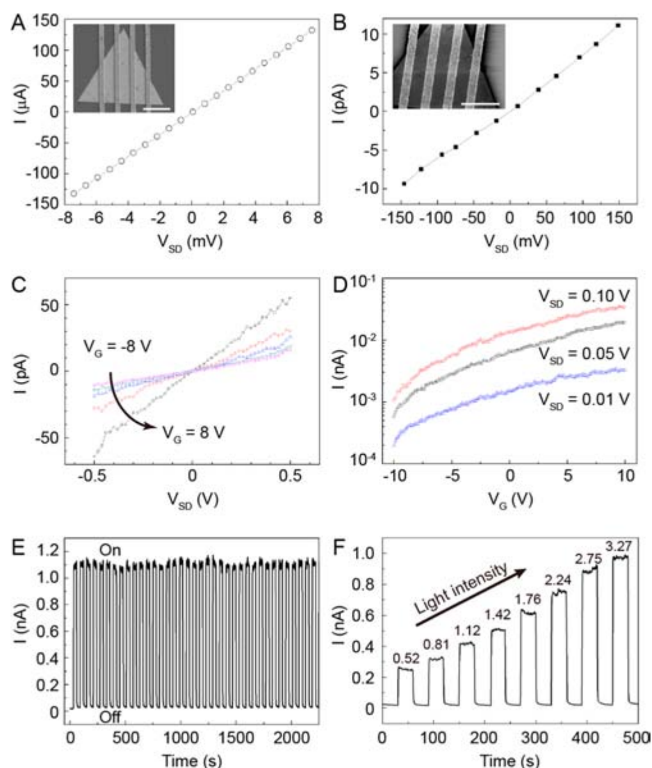

Figure 4. Electronic and photoresponse properties of In_2Se_3 flakes. (A,B) Four-probe $I-V$ curves and the corresponding SEM images of In_2Se_3 flake devices. Scale bars: 5 μm. (C) Output characteristic curves of a semiconducting In_2Se_3 flake at different gate voltages (anticlockwise direction from top to bottom: −8, −4, 0, 4, 8 V). (D) Transfer characteristic curves of the same simple with V_{SD} = 0.01, 0.05, and 0.10 V, respectively. (E) The time trace of source-drain current for the semiconducting In_2Se_3 device when visible light was switched on and off with V_{SD} = 0.1 V and zero gate voltage. (F) Photoresponse of the device with light power increased from 0.52 to 3.27 mW/cm^2 gradually. The corresponding photosensitivity is about 2.5 A/W.

and drain electrodes. The $I-V$ curve of the ~10 QL In_2Se_3 flake with the superlattice phase exhibits metallic behavior with a low resistance of 60 Ω and a high conductivity of ~2.5×10^3 S/cm (Figure 4A).

Interestingly, the measured resistance of the In_2Se_3 flake with the simple hexagonal phase is 1.5×10^{10} Ω (Figure 4B), remarkably larger than that of the superlattice one. Gate voltage-dependent transport measurements of the In_2Se_3 flake with the simple hexagonal phase were also carried out at room temperature. Figure 4C,D shows $I-V$ curves at different gate voltages (V_G) and transfer characteristic curves, respectively. The conductance increased as the V_G swept from negative to positive value, which suggested that In_2Se_3 flake with the single hexagonal lattice is an n-type semiconductor, consistent with bulk In_2Se_3.

Layered In_2Se_3 has a bandgap of 1.26 eV,[17] suitable for visible-light harvest in the solar cells and phototransistors. Figure 4E shows the photoresponse properties of a semiconducting In_2Se_3 flake device. The on−off ratio is ~40 as the light was switched on and off. The on−off switching behavior can be well retained after tens of cycle repeats. Moreover, the output photocurrent increased linearly as incident light power raised (Figures 4F and S4), which suggests that the photocurrent is solely determined by the amount of photogenerated carriers under illumination.[29] Given the measured current of 0.24 nA, the incident light intensity of 0.52 mW/cm^2, and the active area of ~18.4 μm^2, the photosensitivity of atomically thin In_2Se_3 flake is calculated to be ~2.5 A/W (Figure S4), which is superior to the previously reported photosensitivity of pristine graphene (~1 mA/W) and single layer MoS_2 (~7.5 mA/W)[30] and comparable to the value of other mechanically exfoliated 2D GaSe flakes (~2.8 A/W).[31]

In summary, atomically thin In_2Se_3 flakes were successfully synthesized in a controlled manner on layered substrates using van der Waals epitaxy. The thickness, orientation, nucleation site, and crystal phase of as-grown In_2Se_3 flakes were well-controlled by tuning the growth condition for the first time. The atomically thin In_2Se_3 flakes exhibit either semiconducting or metallic behavior depending on the crystal structures. Moreover, transistors based on the semiconducting In_2Se_3 flakes showed an efficient photoresponsivity. The diverse conductivity and efficient photoresponse of In_2Se_3 flakes, combined with selective-area growth make them promising 2D materials for applications in high-performance optoelectronics and phase-change memory devices.

ASSOCIATED CONTENT

Supporting Information

Experimental details and supplementary figures. This material is available free of charge via the Internet at http://pubs.acs.org.

AUTHOR INFORMATION

Corresponding Authors

hlpeng@pku.edu.cn
zfliu@pku.edu.cn

Notes

The authors declare no competing financial interest.

ACKNOWLEDGMENTS

We acknowledge financial support by the National Basic Research Program of China (nos. 2011CB921904, 2013CB932603, 2011CB933003, and 2012CB933404) and the National Natural Science Foundation of China (nos. 21173004, 21222303, 51121091, and 51290272), NCET, and SRF for ROCS, SEM.

REFERENCES

(1) Novoselov, K. S.; Geim, A. K.; Morozov, S. V.; Jiang, D.; Zhang, Y.; Dubonos, S. V.; Grigorieva, I. V.; Firsov, A. A. *Science* **2004**, *306*, 666.

(2) Novoselov, K. S.; Jiang, D.; Schedin, F.; Booth, T. J.; Khotkevich, V. V.; Morozov, S. V.; Geim, A. K. *Proc. Natl. Acad. Sci. U.S.A.* **2005**, *102*, 10451.

(3) Watanabe, K.; Taniguchi, T.; Kanda, H. *Nat. Mater.* **2004**, *3*, 404.

(4) Dean, C. R.; Young, A. F.; Meric, I.; Lee, C.; Wang, L.; Sorgenfrei, S.; Watanabe, K.; Taniguchi, T.; Kim, P.; Shepard, K. L.; Hone, J. *Nat. Nanotechnol.* **2010**, *5*, 722.

(5) Kong, D. S.; Dang, W. H.; Cha, J. J.; Li, H.; Meister, S.; Peng, H. L.; Liu, Z. F.; Cui, Y. *Nano Lett.* **2010**, *10*, 2245.

(6) Li, H.; Cao, J.; Zheng, W.; Chen, Y.; Wu, D.; Dang, W.; Wang, K.; Peng, H. L.; Liu, Z. F. *J. Am. Chem. Soc.* **2012**, *134*, 6132.

(7) Zhang, H.; Liu, C.-X.; Qi, X.-L.; Dai, X.; Fang, Z.; Zhang, S.-C. *Nat. Phys.* **2009**, *5*, 438.

(8) Dang, W.; Peng, H. L.; Li, H.; Wang, P.; Liu, Z. F. *Nano Lett.* **2010**, *10*, 2870.

(9) Wang, Q. H.; Kalantar-Zadeh, K.; Kis, A.; Coleman, J. N.; Strano, M. S. *Nat. Nanotechnol.* **2012**, *7*, 699.

(10) Kwon, S. H.; Ahn, B. T.; Kim, S. K.; Yoon, K. H.; Song, J. *Thin Solid Films* **1998**, *323*, 265.

(11) Park, S. C.; Lee, D. Y.; Ahn, B. T.; Yoon, K. H.; Song, J. *Sol. Energy Mater. Sol. Cells* **2001**, *69*, 99.

(12) Li, Q. L.; Li, Y.; Gao, J.; Wang, S. D.; Sun, X. H. *Appl. Phys. Lett.* **2011**, *99*, 243105.

(13) Zhai, T. Y.; Fang, X. S.; Liao, M. Y.; Xu, X. J.; Li, L.; Liu, B. D.; Koide, Y.; Ma, Y.; Yao, J. N.; Bando, Y.; Golberg, D. *ACS Nano* **2010**, *4*, 1596.

(14) Lee, H.; Kang, D. H.; Tran, L. *Mater. Sci. Eng., B* **2005**, *119*, 196.

(15) Mafi, E.; Soudi, A.; Gu, Y. *J. Phys. Chem. C* **2012**, *116*, 22539.

(16) Julien, C.; Hatzikraniotis, E.; Chevy, A.; Kambas, K. *Mater. Res. Bull.* **1985**, *20*, 287.

(17) Ye, J. P.; Soeda, S.; Nakamura, Y.; Nittono, O. *Jpn. J. Appl. Phys.* **1998**, *37*, 4264.

(18) Popovic, S.; Tonejc, A.; Grzetaplenkovic, B.; Celustka, B.; Trojko, R. *J. Appl. Crystallogr.* **1979**, *12*, 416.

(19) de Groot, C. H.; Moodera, J. S. *J. Appl. Phys.* **2001**, *89*, 4336.

(20) Peng, H. L.; Schoen, D. T.; Meister, S.; Zhang, X. F.; Cui, Y. *J. Am. Chem. Soc.* **2007**, *129*, 34.

(21) Peng, H. L.; Xie, C.; Schoen, D. T.; Cui, Y. *Nano Lett.* **2008**, *8*, 1511.

(22) Lai, K. J.; Peng, H. L.; Kundhikanjana, W.; Schoen, D. T.; Xie, C.; Meister, S.; Cui, Y.; Kelly, M. A.; Shen, Z. X. *Nano Lett.* **2009**, *9*, 1265.

(23) Sun, X. H.; Yu, B.; Ng, G.; Nguyen, T. D.; Meyyappan, M. *Appl. Phys. Lett.* **2006**, *89*, 233121.

(24) Novoselov, K. S.; Fal'ko, V. I.; Colombo, L.; Gellert, P. R.; Schwab, M. G.; Kim, K. *Nature* **2012**, *490*, 192.

(25) Koma, A. *Thin Solid Films* **1992**, *216*, 72.

(26) Koma, A. *J. Cryst. Growth* **1999**, *201*, 236.

(27) Shchukin, V. A.; Bimberg, D. *Rev. Mod. Phys.* **1999**, *71*, 1125.

(28) Jiao, L. Y.; Fan, B.; Xian, X. J.; Wu, Z. Y.; Zhang, J.; Liu, Z. F. *J. Am. Chem. Soc.* **2008**, *130*, 12612.

(29) Sze, S. M. , Ng., K. K. *Physics of Semiconductor Devices*, 3rd ed.; Wiley: New York, 2007.

(30) Yin, Z. Y.; Li, H.; Li, H.; Jiang, L.; Shi, Y. M.; Sun, Y. H.; Lu, G.; Zhang, Q.; Chen, X. D.; Zhang, H. *ACS Nano* **2012**, *6*, 74.

(31) Hu, P. A.; Wen, Z.; Wang, L.; Tan, P.; Xiao, K. *ACS Nano* **2012**, *6*, 5988.